

See discussions, stats, and author profiles for this publication at: <https://www.researchgate.net/publication/50998312>

# Comparative Matrix Isolation Infrared Spectroscopy Study of 1,3- and 1,4-Diene Monoterpenes ( $\alpha$ -Phellandrene and $\gamma$ -Terpinene)

ARTICLE *in* THE JOURNAL OF PHYSICAL CHEMISTRY A · APRIL 2011

Impact Factor: 2.69 · DOI: 10.1021/jp2013122 · Source: PubMed

---

CITATIONS

10

READS

63

---

## 4 AUTHORS:



Katarzyna M Marzec

Jagiellonian University

30 PUBLICATIONS 143 CITATIONS

[SEE PROFILE](#)



Igor D. Reva

University of Coimbra

126 PUBLICATIONS 2,549 CITATIONS

[SEE PROFILE](#)



Rui Fausto

University of Coimbra

330 PUBLICATIONS 4,517 CITATIONS

[SEE PROFILE](#)



Leonard M. Proniewicz

Jagiellonian University

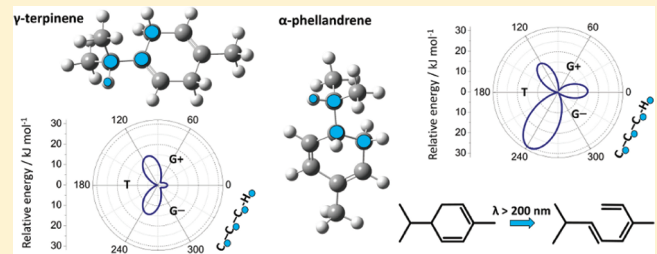
196 PUBLICATIONS 2,434 CITATIONS

[SEE PROFILE](#)

# Comparative Matrix Isolation Infrared Spectroscopy Study of 1,3- and 1,4-Diene Monoterpenes ( $\alpha$ -Phellandrene and $\gamma$ -Terpinene)

K. M. Marzec,<sup>†</sup> I. Reva,<sup>‡</sup> R. Fausto,<sup>\*,‡</sup> and L. M. Proniewicz<sup>\*,§</sup><sup>†</sup>Jagiellonian Centre for Experimental Therapeutics, Jagiellonian University, Bobrzkowskiego 14, 30-348 Krakow, Poland<sup>‡</sup>Department of Chemistry, University of Coimbra, P-3004-535 Coimbra, Portugal<sup>§</sup>Faculty of Chemistry, Jagiellonian University, Ingardena 3, 30-060 Krakow, Poland**S Supporting Information**

**ABSTRACT:** In the present work,  $\gamma$ -terpinene (a 1,4-diene derivative) and  $\alpha$ -phellandrene (1,3-diene derivative) were isolated in cryogenic argon matrices and their structures, vibrational spectra, and photochemistries were characterized with the aid of FTIR spectroscopy and quantum chemical calculations performed at the DFT/B3LYP/6-311++G(d,p) level of approximation. The molecules bear one conformationally relevant internal rotation axis, corresponding to the rotation of the isopropyl group. The calculations provide evidence of three minima on the potential energy surfaces of the studied molecules, where the isopropyl group assumes the trans, gauche+, and gauche- conformations (T, G+, G-). The signatures of all these conformers were identified in the experimental matrix infrared spectra, with the T forms dominating, in agreement with the theoretical predicted abundances in gas phase at room temperature. In situ UV ( $\lambda > 200$  nm) irradiation of matrix-isolated  $\alpha$ -phellandrene led to its isomerization into an open-ring species. The photoproduct was found to exhibit the ZE configuration of its backbone, which to be formed from the reactant molecule does not require extensive structural rearrangements of both the reagent and matrix.  $\gamma$ -Terpinene was photostable when subjected to irradiation under the same experimental conditions. In addition, the liquid compounds at room temperature were also investigated by FTIR-ATR and FT-Raman spectroscopies.



## INTRODUCTION

$\gamma$ -Terpinene (1-isopropyl-4-methyl-1,4-cyclohexadiene; 1) and  $\alpha$ -phellandrene (5-isopropyl-2-methyl-1,3-cyclohexadiene; 2) belong to the group of monocyclic terpenes (Scheme 1) having the molecular formula  $C_{10}H_{16}$  (class of monoterpenes). They are natural products that are isolated from a variety of plant sources.  $\gamma$ -Terpinene has been mainly isolated from citrus fruit oils.<sup>1</sup>  $\alpha$ -Phellandrene is isolated from the plant species *Eucalyptus radiata*. Its name is derived from the plants' former scientific name, *Eucalyptus phellandra*.<sup>2</sup> The growing interest for studying these compounds is mainly related to their bioactivity and odor, which justify their pharmacological, cosmetic, and food uses.<sup>3,4</sup> While  $\gamma$ -terpinene and  $\alpha$ -phellandrene have been determined as components in plants using many quantitative analysis methods,<sup>5–9</sup> they were not studied extensively as main topic compounds.<sup>10</sup>

In  $\alpha$ -phellandrene, the *cis*-1,3-diene fragment inserted in a 6-membered ring is a conjugated  $\pi$  system. On the other hand,  $\gamma$ -terpinene contains two double bonds which are not conjugated (1,4-diene group). As it will be shown in this paper, the presence or absence of the conjugated  $\pi$  system is a fundamental factor in determining the properties of the two compounds and, in particular, their different photochemical behavior.

To the best of our knowledge, the structures of monomeric  $\gamma$ -terpinene and  $\alpha$ -phellandrene have never been reported hitherto.

The crystallographic structure of  $\gamma$ -terpinene was studied at 150 K by the X-ray method.<sup>11</sup> The obtained crystals were orthorhombic, space group *Pnma*,  $Z = 4$ , with  $a = 18.1968(13)$  Å,  $b = 7.2601(5)$  Å,  $c = 6.7498(3)$  Å, and  $\theta = 1.0 \pm 27.5^\circ$ . Within the crystal, the molecules of  $\gamma$ -terpinene assume a conformation where the  $C(H_2)-C-C(CH_3)_2-H$  dihedral angle is  $180^\circ$  (trans; T), and the molecules are stacked along the  $b$  axis and packed in a herring-bone type arrangement. On the other hand, the structure of crystalline  $\alpha$ -phellandrene has not yet been reported.

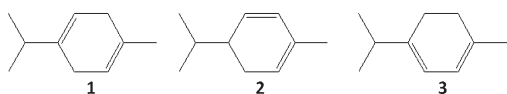
The photochemical behavior of terpenes has been investigated to shed light on decomposition processes that might be relevant for their above-mentioned applications.<sup>12–14</sup> It was found that the UV irradiation of essential plant oils such as those of the tea or lemon tree, under conditions mimicking the natural atmospheric conditions, increases the concentration of *p*-cymene and simultaneously lowers of the amount of other monoterpenoids, such as  $\alpha$ -terpinene,  $\gamma$ -terpinene, terpinolene, and limonene.<sup>14–17</sup> These results suggest that the deterioration process of food products containing  $\gamma$ -terpinene occurs through the sterically favored photooxidation mechanism that leads to conversion of

**Received:** February 9, 2011

**Revised:** March 20, 2011

**Published:** April 04, 2011

**Scheme 1. Structures of  $\gamma$ -Terpinene (1),  $\alpha$ -Phellandrene (2), and  $\alpha$ -Terpinene (3)**



$\gamma$ -terpinene mainly into *p*-cymene.<sup>18</sup> To the best of our knowledge, no data were reported previously on the photochemistry of isolated  $\gamma$ -terpinene. On the other hand, the photochemistry of  $\alpha$ -phellandrene was investigated before using ab initio multistate second-order perturbation theory and gas-phase femtosecond time-resolved spectroscopy,<sup>19</sup> where it was shown that  $\alpha$ -phellandrene may undergo the ring-opening conversion leading to the cyclohexatriene-type product.

The two title molecules are isomers of  $\alpha$ -terpinene (3, in Scheme 1), which was the subject of our previous investigation.<sup>12</sup> Like  $\alpha$ -phellandrene,  $\alpha$ -terpinene contains also a *cis*-1,3-diene conjugated fragment inserted in a 6-membered ring. UV ( $\lambda > 235$  nm) irradiation of matrix-isolated  $\alpha$ -terpinene led to its isomerization into an open-ring species, 2,6-dimethyl-5-methylenehepta-1,3-diene, in a concerted  $\sigma^2 + \pi^4$  electrocyclic ring-opening reaction, the photoproduct being generated in the *Z* configuration around the central  $C_3=C_4$  double bond and in conformations requiring the smallest structural rearrangements of both the reagent and matrix. The photochemistry of  $\alpha$ -phellandrene and  $\alpha$ -terpinene parent molecule, 1,3-cyclohexadiene, was also previously investigated by several theoretical and experimental methods.<sup>19–24</sup> It has been found that 1,3-cyclohexadiene undergoes exclusively the ring-opening photoreaction.<sup>25</sup> It was also found experimentally that  $\alpha$ -phellandrene in solutions may undergo similar ring-opening reactions<sup>26</sup> as well as other types of isomerizations.<sup>27</sup>

In the present work, a detailed investigation of the structure, spectroscopy, and photochemistry of  $\gamma$ -terpinene and  $\alpha$ -phellandrene is reported. The monomers of these compounds were isolated in cryogenic argon matrices, their structures characterized and the corresponding infrared spectra interpreted and assigned. In addition, in situ UV irradiation of the matrix-isolated compounds was performed, and their photochemistries probed by FTIR spectroscopy. The neat liquid substances, at room temperature, were also investigated by FTIR-ATR and FT-Raman spectroscopies. The experimental studies were complemented by quantum chemical calculations, which allowed for a detailed characterization of the conformational space of the two molecules and identification of the spectroscopically observed photoproducts.

## ■ EXPERIMENTAL AND COMPUTATIONAL METHODS

$\gamma$ -Terpinene and  $\alpha$ -phellandrene were provided by Fluka (purum,  $\geq 98.5\%$  (GC) and  $\geq 95.0\%$  (GC), respectively). The matrix gas, argon N60, was supplied by Air Liquide.

The low-temperature equipment was based on an APD Cryogenics closed-cycle helium refrigerator with a DE-202A expander. For preparation of the matrices, the studied compound ( $\alpha$ -phellandrene or  $\gamma$ -terpinene) and argon were premixed in a molar ratio of ca. 1:500, and deposited through a needle valve. The valve nozzle was kept at room temperature, which defined the conformational distribution in the gas phase prior to deposition. The temperature of the cold CsI window of the cryostat was kept at about 13 K and was measured directly at the sample holder by a silicon diode temperature sensor, connected to a

digital temperature controller (Scientific Instruments, Model 9650-1), which provides an accuracy of 0.1 K. The matrix isolation IR spectra were collected on a Nicolet 6700 FTIR spectrometer, equipped with a deuterated triglycine sulfate (DTGS) detector and a Ge/KBr beam splitter, with  $0.5\text{ cm}^{-1}$  spectral resolution.

The matrices were irradiated (180 min for  $\gamma$ -terpinene and 330 min for  $\alpha$ -phellandrene) using a 200 W output power of a 300 W Hg/Xe lamp (Oriel, Newport) and a series of long-pass optical filters, through the quartz ( $\lambda > 200$  nm) or KBr ( $\lambda > 235$  nm) external windows of the cryostat.

The room temperature FTIR-ATR spectra ( $650\text{--}4000\text{ cm}^{-1}$ ) of the liquid compounds (ca.  $5\text{--}10\text{ }\mu\text{L}$  of sample placed on the surface of a diamond-ZnSe ATR crystal with 0.5 mm diameter) were recorded using a portable diamond TravelIR spectrometer, fitted with a deuterated L-alanine-doped triglycine sulfate (DLATGS) detector, in a single reflection configuration. Sixteen scans, with a spectral resolution of  $4\text{ cm}^{-1}$ , were accumulated.

The Raman spectra of the liquid compounds were recorded at room temperature on a Nicolet NXR 9650 FT-Raman spectrometer, equipped with a Nd<sup>3+</sup>:YAG laser, emitting at 1064 nm ( $9398.5\text{ cm}^{-1}$ ), and a germanium detector cooled with liquid nitrogen. The laser power at the sample position was 100 mW. 512 scans with a resolution of  $4\text{ cm}^{-1}$  were collected and averaged.

Density functional theory (DFT) calculations were carried out using the Gaussian 09<sup>28</sup> program package. The geometries of the conformers of  $\alpha$ -phellandrene and  $\gamma$ -terpinene as well as possible photoproducts were fully optimized at the B3LYP/6-311++G-(d,p) level of theory.<sup>29</sup> Additionally, the influence of a polar environment on the stability of the minima was estimated using the conductor-like polarized continuum C-PCM approach (PCM) at the same level of theory, with toluene as a solvent.<sup>30,31</sup>

Theoretical Raman intensities ( $I_i$ ) were obtained from the Gaussian calculated Raman scattering activities ( $S_i$ ) according to the expression  $I_i = 10^{-12}(\nu_0 - \nu_i)^4\nu_i^{-1}B_i^{-1}S_i$ , where  $B_i$  is a temperature factor which accounts for the intensity contribution of excited vibrational states and is represented by the Boltzmann distribution [ $B_i = 1 - \exp\{-(h\nu_i c)/(kT)\}$ ];  $h$ ,  $k$ ,  $c$ , and  $T$  are Planck and Boltzmann constants, speed of light, and temperature in kelvin, respectively;  $\nu_0$  is the frequency of the laser excitation line ( $\nu_0 = 1/\lambda_0$ , where  $\lambda_0$  is the laser wavelength);  $\nu_i$  is the frequency of normal mode.<sup>32</sup>

Prior to the comparison of the calculated wavenumbers with their experimental counterparts (IR and Raman spectra), the first were scaled down by appropriate scale factors (0.978 and 0.960 for the  $0\text{--}2000$  and  $2000\text{--}4000\text{ cm}^{-1}$  regions, respectively<sup>33,34</sup>), mainly to account for anharmonicity effects, basis set truncation, and the neglected part of electron correlation. To provide an unequivocal assignment of the calculated IR and Raman spectra, normal-coordinate analysis calculations were performed using a set of internal coordinates defined as suggested by Pulay, Fogarasi and co-authors.<sup>35,36</sup> Program GAR2PED was used for calculation of potential energy distribution (PED) of normal modes in terms of natural internal coordinates.<sup>37</sup>

## ■ RESULTS AND DISCUSSION

**Conformational Space of  $\gamma$ -Terpinene and  $\alpha$ -Phellandrene.** The molecule of  $\alpha$ -phellandrene has one chiral center, carbon atom C2 (see Figure 1 for atom numbering). The geometric parameters of  $\alpha$ -phellandrene reported in this work refer to the S-enantiomer.  $\alpha$ -Phellandrene has two conformationally relevant internal rotation

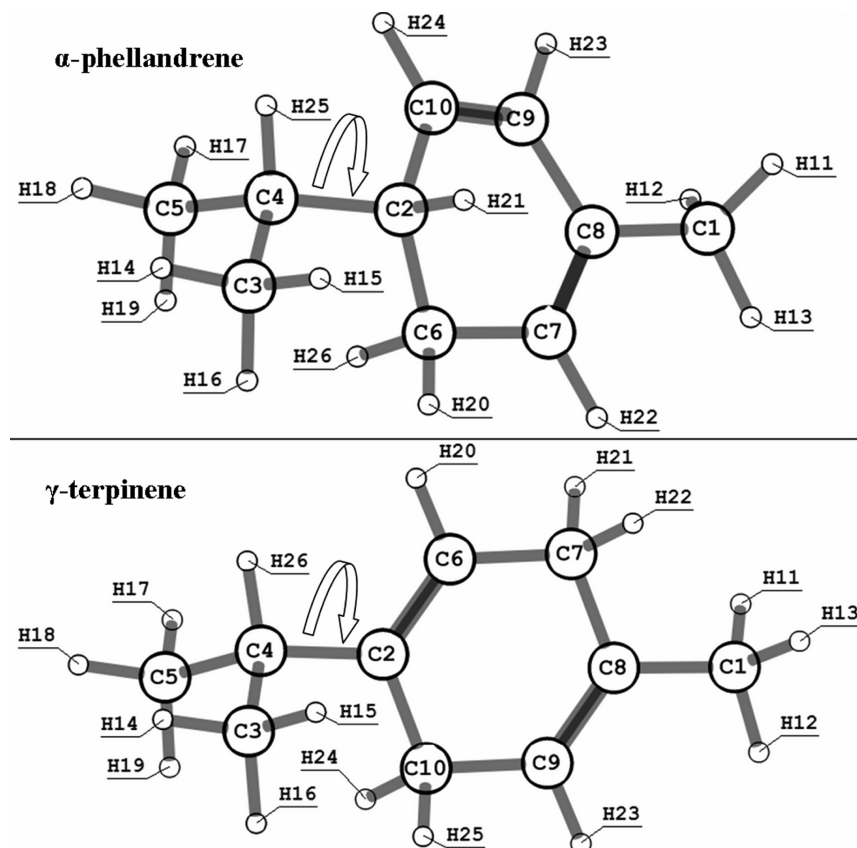


**Figure 1.** Trans conformers of  $\alpha$ -phellandrene (top) and  $\gamma$ -terpinene (bottom) with atom numbering. The conformers are named according to the value of the  $C_{10}-C_2-C_4-H_{26}$  ( $\gamma$ -terpinene) or  $C_6-C_2-C_4-H_{25}$  ( $\alpha$ -phellandrene) dihedral angle (see arrows in the figure), defining the orientation of the isopropyl group in relation to the ring. The dihedral angle  $C_6-C_2-C_4-H_{25}$  ( $\alpha$ -phellandrene) for T, G+, and G- is equal to  $179.6^\circ$ ,  $69.6^\circ$ , and  $-48.1^\circ$ , respectively. The dihedral angle  $C_{10}-C_2-C_4-H_{26}$  ( $\gamma$ -terpinene) for T, G+, and G- is equal to  $180.0^\circ$ ,  $47.5^\circ$ , and  $-47.5^\circ$ , respectively.

**Table 1.** DFT(B3LYP)/6-311++G(d,p) Calculated Relative Energies without ( $\Delta E^\circ$ ) and with ( $\Delta E^\circ_{ZPVE}$ ) Zero-Point Corrections, Relative Gibbs Energies at 298 K ( $\Delta G^\circ$ ), and Dipole Moments ( $|\mu|$ ) of  $\gamma$ -Terpinene and  $\alpha$ -Phellandrene Conformers<sup>a</sup>

compound	conformer	$\Delta E^\circ$	$\Delta E^\circ_{ZPVE}$	$\Delta G^\circ$	$ \mu $
$\gamma$ -terpinene	trans (T)	0.00	0.00	0.00	0.07
	gauche (G±)	1.73	1.78	1.77	0.05
$\alpha$ -phellandrene	trans (T)	0.00	0.00	0.00	0.23
	gauche (G+)	0.80	1.00	1.06	0.21
	gauche (G-)	0.42	0.37	0.27	0.29

<sup>a</sup> Energies in  $\text{kJ mol}^{-1}$ . The absolute energies (all in hartrees; 1 hartree  $\approx 2625.5 \text{ kJ mol}^{-1}$ ) of the most stable conformer for  $\gamma$ -terpinene are  $\Delta E^\circ = -390.788\,785$ ,  $\Delta E^\circ_{ZPVE} = -390.555\,543$ , and  $\Delta G^\circ$  (at 298.15 K) =  $-390.592\,109$ ; for  $\alpha$ -phellandrene they are  $-390.783\,951$ ,  $-390.550\,626$ , and  $-390.586\,473$ , respectively. Dipole moments in debyes.

axes: (i) rotation of the isopropyl group in relation to the ring and (ii) twist of the ring, which can be described by the orientation of the dihedral angle around the two neighboring sp<sup>3</sup> carbon atoms of the ring ( $C_{10}-C_2-C_6-C_7$ ). The second parameter can assume two values, gauche+ and gauche-, producing two equivalent-by-symmetry geometries of the ring subunit. In the present study, only gauche- orientation of the ring was considered. In all minima

found, this parameter was very rigid, falling in a narrow range of values from  $-44^\circ$  to  $-46^\circ$ . Therefore, the unique set of conformers of  $\alpha$ -phellandrene can be defined by a single parameter, that is, by the internal rotation of the isopropyl group.

The molecule of  $\gamma$ -terpinene does not have chiral centers. Furthermore, the two sp<sup>3</sup> carbon atoms of its ring are separated by two sp<sup>2</sup> carbon atoms from each side, thus allowing for the planar arrangement of the ring. Indeed, in all the found structures of  $\gamma$ -terpinene minima the ring subunit is essentially planar. Then,  $\gamma$ -terpinene has only one conformationally relevant internal rotation axis, which corresponds to the rotation of the isopropyl group in relation to the ring.

The DFT calculations led to the identification of three minima on the potential energy surface of each molecule, corresponding to the trans, gauche+, and gauche- conformers (Figure 1). The conformers of  $\alpha$ -phellandrene are named here according to the orientation of the  $C_6-C_2-C_4-H_{25}$  dihedral angle, while for  $\gamma$ -terpinene according to the orientation of the  $C_{10}-C_2-C_4-H_{26}$  dihedral angle. In  $\alpha$ -phellandrene, the three unique forms, trans ( $179.6^\circ$ ), gauche+ ( $69.6^\circ$ ), and gauche- ( $-48.1^\circ$ ), belong to the  $C_1$  symmetry point group. In  $\gamma$ -terpinene, the trans ( $180.0^\circ$ ) conformer has  $C_s$  symmetry, while the gauche+ ( $47.5^\circ$ ) and gauche- ( $-47.5^\circ$ ) conformers ( $C_1$  symmetry) are mirror images. The optimized geometries of these conformers are given in Table S1 (Supporting Information), whereas the values of relative energies and dipole moments are presented in Table 1.

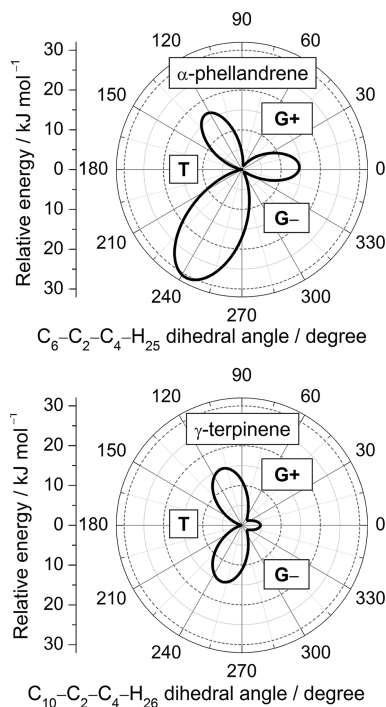


**Figure 2.** DFT(B3LYP)/6-311++G(d,p) calculated potential energy (radial coordinate) profiles for interconversion between the conformers of (top)  $\alpha$ -phellandrene and (bottom)  $\gamma$ -terpinene. Minima are labeled by the conformer symbol (see Figure 1). Each profile was obtained by performing a relaxed scan along the conformationally relevant torsional coordinate of the molecule ( $C_6-C_2-C_4-H_{25}$  for  $\alpha$ -phellandrene and  $C_{10}-C_2-C_4-H_{26}$  for  $\gamma$ -terpinene; dihedral angles defining the internal rotation of the isopropyl group), by varying this coordinate in steps of  $10^\circ$  and optimizing all the remaining internal coordinates.

For both compounds, the most stable conformer is the trans (T) form. In the case of  $\gamma$ -terpinene, the two gauche conformers ( $G\pm$ ) are degenerate by symmetry and were calculated to be  $1.78\text{ kJ mol}^{-1}$  higher in energy than the trans form (zero-point-corrected energies). In  $\alpha$ -phellandrene,  $G+$  and  $G-$  are calculated to be  $1.00$  and  $0.37\text{ kJ mol}^{-1}$  higher in energy than T, respectively.

The calculated potential energy profiles for interconversion between the three conformers of the studied compounds (Figure 2) show that the barriers for  $T \rightarrow G\pm$  and  $G\pm \rightarrow G\pm$  isomerizations in  $\gamma$ -terpinene amount to ca.  $15$  and  $3\text{ kJ mol}^{-1}$ , respectively. In  $\alpha$ -phellandrene, the  $T \rightarrow G+$ ,  $G+ \rightarrow G-$ , and  $T \rightarrow G-$  barriers are predicted as  $17$ ,  $14$ , and  $32\text{ kJ mol}^{-1}$ , respectively. These results are particularly relevant for the interpretation of the matrix isolation experiments presented later in this paper. Indeed, all relevant barriers are high and the conversion between the conformers during their landing and cooling on the surface of the optical substrate during deposition of the matrices can be neglected. [The  $G+ \leftrightarrow G-$  barrier in  $\gamma$ -terpinene is low, but interconversion between the two equivalent-by-symmetry gauche forms is irrelevant for the performed spectroscopic experiments, since their spectra are equal.] Because, the matrices presented here were obtained from the vapor of the compounds at room temperature, one can assume that the relative populations of the conformers trapped into the matrices should reflect the conformational equilibrium in the gas phase at that temperature. The  $G\pm:T$  population ratio for  $\gamma$ -terpinene

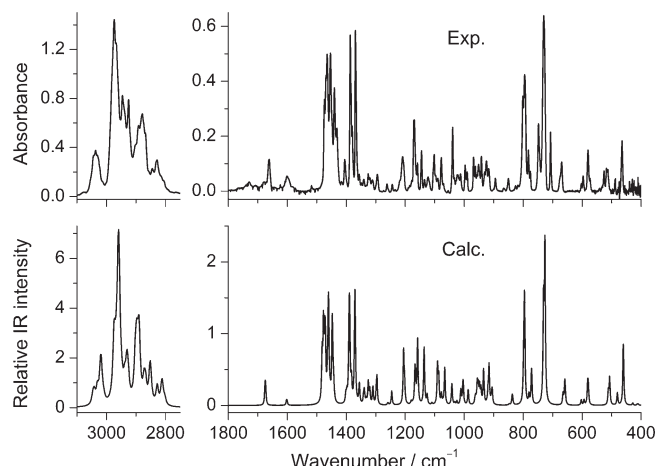


**Figure 3.** (Top) Experimental FTIR spectra of  $\alpha$ -phellandrene embedded in argon (diluted matrix, 13 K). (Bottom) Simulated spectrum obtained as a sum of theoretical infrared spectra of  $\alpha$ -phellandrene conformers with their intensities scaled proportionally to their estimated room-temperature gas-phase populations ( $G+/G-/T$  is  $25.6:35.2:39.2$ ). The theoretical spectra in the CH stretching ( $3100-2750\text{ cm}^{-1}$ ) and fingerprint ( $1800-400\text{ cm}^{-1}$ ) regions were simulated by Lorentzian functions centered at the DFT(B3LYP)/6-311++G(d,p) calculated wavenumbers scaled by  $0.960$  and  $0.978$ , respectively, and with fwhm equal to  $10$  and  $4\text{ cm}^{-1}$ , respectively.

trapped in the argon matrices should then be  $49.5\%:50.5\%$  (i.e.,  $\sim 1:1$ ), as estimated from the calculated relative Gibbs free energies at  $298.15\text{ K}$  of the conformers using the Boltzmann statistics, while in  $\alpha$ -phellandrene the  $G+:G-:T$  population ratio should be  $25.6\%:35.2\%:39.2\%$  (i.e.,  $\sim 0.65:0.9:1$ ).

**Infrared Spectra of the As-Deposited Matrices of  $\gamma$ -Terpinene and  $\alpha$ -Phellandrene.** The infrared spectra of the as-deposited argon matrices of the studied compounds are shown in Figures 3 and 4. These spectra are compared with the simulated spectra of the compounds obtained by adding the DFT calculated infrared spectra of the individual conformers of each molecule with intensities scaled by factors proportional to their estimated populations.

The good agreement between the experimentally observed spectra and their simulated counterparts confirms the presence in the matrices of the two conformers of  $\gamma$ -terpinene (T,  $G\pm$ ) and the three conformers of  $\alpha$ -phellandrene (T,  $G+$ ,  $G-$ ) predicted theoretically. The detailed assignment of the spectra is shown in Tables S2–S5 (Supporting Information).

In the more detailed analysis of the spectra presented below, we focus on only three spectral regions. These regions contribute to the identification of the individual conformers in the matrices ( $1200-1000\text{ cm}^{-1}$ ) or are related to the molecular fragments which are expected to be directly involved in the photochemical processes described in detail later (in particular, C=C stretching and CH out-of-plane modes).

According to the previously observed photoreactions of the analogous molecules,  $\alpha$ -terpinene<sup>12</sup> and 1,3-cyclohexadiene,<sup>25</sup> the photochemical excitation of the studied compounds can be expected to strongly affect the  $\pi$  system of their rings. Then, the C=C stretching vibrations appear as good probes of the photochemical events. In addition to the C=C stretching vibrations, the out-of-plane deformation vibrations of the C–H groups, specifically those in which the carbon atom is involved in a double bond ( $sp^2$  carbon atoms), are very sensitive to changes in the  $\pi$  system and rearrangements of the rings. These vibrations were also shown

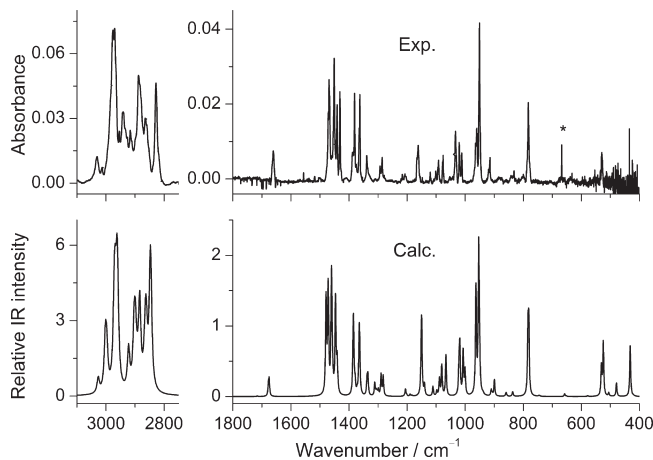


**Figure 4.** (Top) Experimental FTIR spectra of  $\gamma$ -terpinene embedded in argon (diluted matrix, 13 K). (Bottom) Simulated spectrum obtained as a sum of theoretical infrared spectra of  $\gamma$ -terpinene conformers with their intensities scaled proportionally to their estimated room-temperature gas-phase populations (G/T is 49.5:50.5). The theoretical spectra in the CH stretching ( $3100\text{--}2750\text{ cm}^{-1}$ ) and fingerprint ( $1800\text{--}400\text{ cm}^{-1}$ ) regions were simulated by Lorentzian functions centered at the DFT(B3LYP)/6-311++G(d,p) calculated wavenumbers scaled by 0.960 and 0.978, respectively, and with fwhm equal to 10 and  $4\text{ cm}^{-1}$ , respectively. An asterisk designates the band due to the atmospheric  $\text{CO}_2$ .

previously to be useful to identify the type of photoreactions observed due to UV irradiation of this type of compounds.<sup>12</sup>

The vibrations of the C=C bonds are expected to give rise to bands in a spectral region free from other bands originated in the compounds. The antisymmetric stretching vibration of the conjugated C=C bonds of the  $\alpha$ -phellandrene ring are calculated at 1675, 1676, and  $1673\text{ cm}^{-1}$  for conformers T, G+, and G-, respectively, and observed in the experimental IR spectra at  $1663\text{ cm}^{-1}$  as a medium-intensity band (Figure 3). In turn, the C=C symmetric stretching vibration is predicted at  $1603\text{ cm}^{-1}$  in both T and G+ conformers and at  $1601\text{ cm}^{-1}$  in G-, being observed experimentally at  $1601\text{ cm}^{-1}$ . This relatively weak IR band is strong in the Raman spectrum of this compound in the liquid state, where it is observed at  $1590\text{ cm}^{-1}$  (see Table S3 and Figure S1 in the Supporting Information).

In the case of  $\gamma$ -terpinene, the order of frequencies of the two C=C stretching modes is reversed compared to  $\alpha$ -phellandrene. The C=C antisymmetric stretching is calculated at 1675 and  $1678\text{ cm}^{-1}$  for T and G $\pm$  conformers, respectively, and observed at  $1670\text{ cm}^{-1}$  (Figure 4). The C=C symmetric stretching is predicted at ca.  $1715\text{ cm}^{-1}$  with a very low intensity in the infrared ( $<0.1\text{ km mol}^{-1}$ ) and could not be observed in the experimental spectrum of the matrix isolated compound. However, as in the case of  $\alpha$ -phellandrene, this mode gives rise to a very strong band in the Raman spectrum of the liquid compound, where it appears at  $1701\text{ cm}^{-1}$  (see Table S5 and Figure S1 in the Supporting Information).

The reason for the different order of frequencies of the C=C stretching vibrations in  $\gamma$ -terpinene and  $\alpha$ -phellandrene results from the different composition of these modes in the two molecules, as shown in the potential energy distribution results presented in Tables S3 and S5 in the Supporting Information. In  $\alpha$ -phellandrene, the highest contribution to the antisymmetric stretching comes from the  $\text{C}_7=\text{C}_8$  bond (adjacent to the methyl

group), while for  $\gamma$ -terpinene the highest percent contribution is connected with the  $\text{C}_2=\text{C}_6$  bond (adjacent to the isopropyl group). The situation is inverse regarding the compositions of the C=C symmetric stretching in the two molecules. The contributions of the individual double bonds to the antisymmetric stretching C=C vibration amount to 45–47% ( $\nu(\text{C}_7\text{C}_8)$ ) + 22–23% ( $\nu(\text{C}_9\text{C}_{10})$ ) for  $\alpha$ -phellandrene, and 23–25% ( $\nu(\text{C}_8\text{C}_9)$ ) + 48–50% ( $\nu(\text{C}_2\text{C}_6)$ ) for  $\gamma$ -terpinene. The corresponding symmetric C=C vibrations are composed as 23–24% ( $\nu(\text{C}_7\text{C}_8)$ ) + 48–49% ( $\nu(\text{C}_9\text{C}_{10})$ ) for  $\alpha$ -phellandrene, and 46–47% ( $\nu(\text{C}_8\text{C}_9)$ ) + 22–23% ( $\nu(\text{C}_2\text{C}_6)$ ) for  $\gamma$ -terpinene (see Tables S3 and S5).

Regarding the C–H deformations, three of such vibrations are expected for  $\alpha$ -phellandrene, according to the number of the CH groups linked to the ring. One of the CH groups is attached to the double C=C bond bearing the methyl group on the other side. The deformation vibration of this CH group ( $\omega(\text{C}_7\text{H}_{22})$ ) is uncoupled from the other two CH groups and is related with an intense IR band observed at  $795\text{ cm}^{-1}$  (calculated  $795\text{--}798\text{ cm}^{-1}$ , 77–80% PED). The out-of-plane vibrations of the other two CH groups ( $\omega(\text{C}_9\text{H}_{23})$ ,  $\omega(\text{C}_{10}\text{H}_{24})$ ), making part of the  $\text{C}=\text{CH}-\text{CH}=\text{C}$  fragment of the molecule, are coupled in the symmetric and antisymmetric ways. The symmetric combination is related with the most intense IR band in the entire fingerprint region (calculated intensity  $21\text{--}23\text{ km mol}^{-1}$ ) appearing at  $730\text{ cm}^{-1}$  (calculated  $726\text{--}731\text{ cm}^{-1}$ , 62–63% PED). The antisymmetric combination gives origin to a weak IR absorption (calculated intensity  $\sim 1\text{ km mol}^{-1}$ ) in the  $962\text{--}968\text{ cm}^{-1}$  range (calculated  $959\text{--}964\text{ cm}^{-1}$ , 63–84% PED).

In the case of  $\gamma$ -terpinene, only two CH groups are linked to the ring. Like in  $\alpha$ -phellandrene, it is expected that their out-of-plane vibrations are coupled and their symmetric and antisymmetric combinations should give a strong and a weak absorption in infrared. Indeed, a strong (symmetric) infrared band is observed at  $783\text{ cm}^{-1}$  (calculated  $781\text{--}784\text{ cm}^{-1}$ ,  $\omega(\text{C}_9\text{H}_{23})$  35–37% PED, and  $\omega(\text{C}_6\text{H}_{20})$  10–11% PED) and a weak (antisymmetric) band appears at  $832\text{ cm}^{-1}$  ( $836\text{--}837\text{ cm}^{-1}$ ,  $\omega(\text{C}_6\text{H}_{20})$  52–58% PED, and  $\omega(\text{C}_9\text{H}_{23})$  25–27% PED). These two coordinates are partially mixed with the rocking motion of the two methylene groups linked to the ring. These mixtures give rise to two more infrared bands (medium and strong intensity) both in the  $950\text{--}965\text{ cm}^{-1}$  spectral range (see Table S5), i.e., in the same range as for the out-of-plane CH vibrations in  $\alpha$ -phellandrene (see Table S3).

The conformer-sensitive range in the IR spectra of  $\gamma$ -terpinene and  $\alpha$ -phellandrene extends from  $1200$  to  $1000\text{ cm}^{-1}$  (Figures 5 and 6; see also Tables S3 and S5 in the Supporting Information for results of normal-coordinate analysis). In the case of  $\gamma$ -terpinene (see Figure 5), the assignments are doubtless and could be made easily. In the considered region, the bands observed at  $1012\text{ cm}^{-1}$  (delocalized vibration with a considerable degree of the stretching of the  $\text{C}_2-\text{C}(\text{CH}_3)_2$  bond; calculated  $1001\text{ cm}^{-1}$ ),  $1076\text{ cm}^{-1}$  (stretching of the  $\text{C}_9-\text{C}_{10}$  bond; calculated  $1067\text{ cm}^{-1}$ ),  $1101\text{ cm}^{-1}$  (C–C antisymmetric stretching of the isopropyl moiety; calculated  $1089\text{ cm}^{-1}$ ),  $1148\text{ cm}^{-1}$  (extensively mixed vibration delocalized over the whole molecule; calculated  $1141\text{ cm}^{-1}$ ) and  $1162\text{ cm}^{-1}$  (predominantly  $\text{C}_8-\text{CH}_3$  bond; calculated  $1150\text{ cm}^{-1}$ ) are marks of the trans (T) conformer. On the other hand, the bands appearing at  $1021\text{ cm}^{-1}$  (mostly the symmetric stretching of the  $\text{C}_6-\text{C}_7$  and  $\text{C}_9-\text{C}_{10}$  bonds; calculated  $1008\text{ cm}^{-1}$ ),  $1092\text{ cm}^{-1}$  (antisymmetric stretching of the  $\text{C}_6-\text{C}_7$  and  $\text{C}_9-\text{C}_{10}$  bonds;

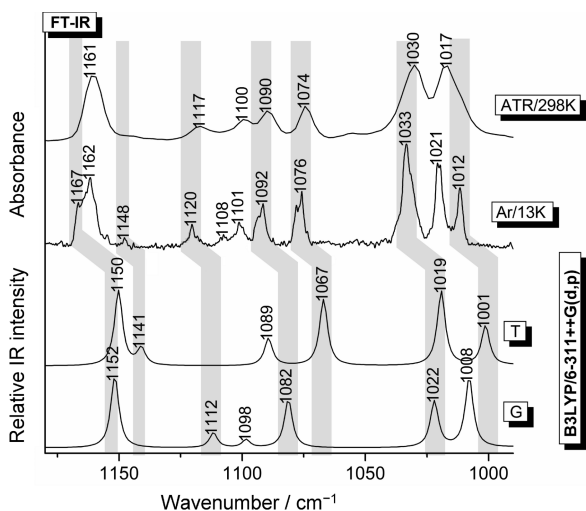


**Figure 5.** Comparison of the FTIR spectrum of  $\gamma$ -terpinene isolated in an argon matrix, its FTIR-ATR spectrum in liquid phase at 298 K, and the calculated IR spectra of T and G $\pm$  conformers. The theoretical spectra were calculated at the DFT(B3LYP)/6-311++G(d,p) level of theory, and wavenumbers were scaled by a factor of 0.978. Absorption bands were simulated with Gaussian profiles, centered at the calculated (scaled) wavenumbers and having fwhm of 4 cm<sup>-1</sup>.

calculated 1082 cm<sup>-1</sup>), 1108, 1120, and 1167 cm<sup>-1</sup> (all extensively mixed vibrations with predominant contribution from the C<sub>2</sub>—C(CH<sub>3</sub>)<sub>2</sub> stretching coordinate; calculated at 1098, 1112, and 1152 cm<sup>-1</sup>, respectively) belong to the gauche forms (G $\pm$ ), and the strong band at 1033 cm<sup>-1</sup> contains contributions from both forms (predominantly C<sub>6</sub>—C<sub>7</sub> stretching; calculated 1019 cm<sup>-1</sup> T, 1022 cm<sup>-1</sup> G $\pm$ ).

The analysis of the data in the case of  $\alpha$ -phellandrene (Figure 6) is more complicated, because of the larger number of conformers, leading to a substantial increase in the complexity of the experimental spectra. According to the predicted relative conformational populations presented in the previous section, the IR spectrum of matrix-isolated  $\alpha$ -phellandrene is dominated by the bands due to the T and G $-$  conformers, which are expected to be present in the argon matrix with larger populations. The bands assigned only to T conformer are observed at 1078, 1100, and 1135 cm<sup>-1</sup>, and are ascribed to vibrations with dominant contributions of the C<sub>6</sub>—C<sub>7</sub>, isopropyl C—C antisymmetric, and C<sub>2</sub>—C<sub>6</sub> stretching coordinates, respectively, which were calculated at 1067, 1088, and 1166 cm<sup>-1</sup>. Those due to G $-$  form only are the bands observed at 1024, 1102, 1145, and 1171 cm<sup>-1</sup>, which correspond to the calculated bands at 1012, 1091, 1136, and 1168 cm<sup>-1</sup>, with substantial contributions from the C<sub>2</sub>—C<sub>6</sub>, isopropyl C—C antisymmetric, isopropyl group rocking coordinates, and in-plane H<sub>23</sub>—C<sub>9</sub>=C<sub>10</sub>—H<sub>24</sub> deformation, respectively. Finally, the bands observed at 1120 (shoulder) and 1123 cm<sup>-1</sup> are due to G $+$  (C<sub>2</sub>—C(CH<sub>3</sub>)<sub>2</sub> and isopropyl C—C antisymmetric stretching modes; calculated wavenumbers: 1110 and 1127 cm<sup>-1</sup>). The remaining bands appearing in this spectral range contain contributions from more than one conformer, e.g., bands at 1013 and 1090 cm<sup>-1</sup> from G $+$  and G $-$ , the band at 1030 cm<sup>-1</sup> from T and G $+$ , and those at 1039 and 1159 cm<sup>-1</sup> from all three forms.

The FTIR-ATR spectrum of liquid  $\gamma$ -terpinene (see Figure 5) compares well with the matrix isolation spectrum of the compound, the main difference being the expected band broadening,

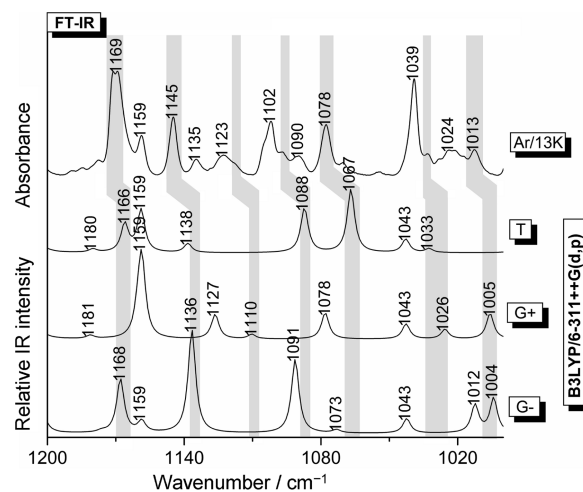


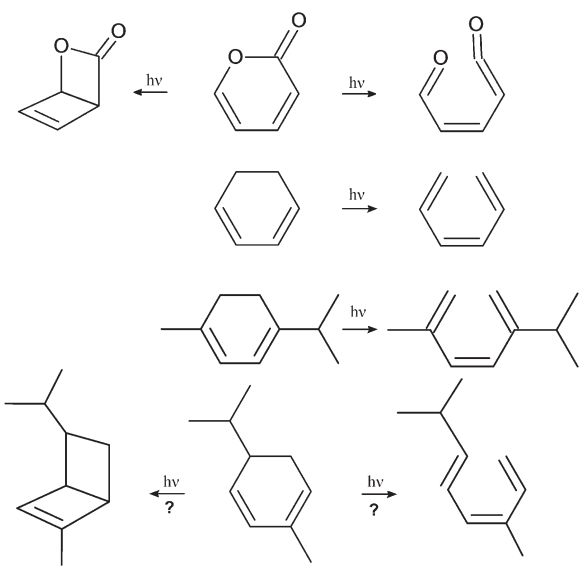
**Figure 6.** Comparison of the FTIR spectrum of  $\alpha$ -phellandrene isolated in an argon matrix with the calculated IR spectra of T, G $+$ , and G $-$  conformers. The theoretical spectra were calculated at the DFT(B3LYP)/6-311++G(d,p) level of theory, and wavenumbers were scaled by a factor of 0.978. Absorption bands were simulated with Gaussian profiles, centered at the calculated (scaled) wavenumbers and having fwhm of 4 cm<sup>-1</sup>.

pointing to a similar equilibrium conformational composition in both the gas and liquid phase of the compound at room temperature. In the case of  $\alpha$ -phellandrene the liquid-phase FTIR-ATR spectrum is also composed by broad bands and is shown in Figure S1 (Supporting Information). The comparison between the experimental FT-Raman spectra of the two compounds at room temperature and the theoretical Raman spectra of their conformers in the conformer-sensitive region (1200–1000 cm<sup>-1</sup>, Figure S1) shows also that the population of the conformers in the liquid at room temperature is similar to the population in the gas phase at the same temperature. This result could be anticipated, considering the similar values of the dipole moments for the different conformers of each molecule (see Table 1).

**Photochemical Processes and Analysis of the Photoproducts.** Scheme 2 summarizes the experimentally observed photochemistry of compounds analogous to  $\alpha$ -phellandrene which have a *cis*-1,3-diene fragment inserted in a six-membered ring:  $\alpha$ -terpinene,<sup>12</sup> 1,3-cyclohexadiene,<sup>25</sup> and  $\alpha$ -pyrone.<sup>38</sup> In the last case, besides the ring-opening reaction, isomerization to the  $\alpha$ -pyrone Dewar form was also observed. Bearing the same conjugated  $\pi$ -system,  $\alpha$ -phellandrene can be expected to show a similar photochemistry, as represented in Scheme 2. On the other hand,  $\gamma$ -terpinene has a different arrangement of the double bonds in the ring (the 1,4-diene moiety), and despite its UV spectrum not differing very much from those of compounds with *cis*-1,3-diene fragment (Figure S2 in the Supporting Information), it can be expected to behave differently when exposed to UV light.

The matrix-isolated  $\alpha$ -phellandrene and  $\gamma$ -terpinene were subjected to a series of UV irradiations using different cutoff filters. For irradiations with wavelengths longer than 288 nm, no changes were observed in the infrared spectrum of  $\alpha$ -phellandrene. This is consistent with the UV absorption spectrum of the compound (Figure S2) as well as with that of the parent molecule 1,3-cyclohexadiene,<sup>19,39</sup> both compounds not absorbing above 280 nm. On the other hand, irradiation at  $\lambda > 200$  nm

**Scheme 2. Experimentally Observed Photochemistries for (Top to Bottom)  $\alpha$ -Pyrone,<sup>38</sup> 1,3-Cyclohexadiene,<sup>25</sup> and  $\alpha$ -Terpinene,<sup>12</sup> and the Possible Analogous Photoreactions of  $\alpha$ -Phellandrene**



(where  $\alpha$ -phellandrene, 1,3-cyclohexadiene, and  $\alpha$ -terpinene exhibit their main absorptions) led to the emergence of new bands in the infrared spectrum of the irradiated matrix of  $\alpha$ -phellandrene. These results show that  $\alpha$ -phellandrene is photolabile in the range of germicidal UV-C light only. No changes were observed in the infrared spectrum of the irradiated  $\gamma$ -terpinene matrix in the whole range of wavelengths used in our experiments. This result demonstrates the relevance of the different arrangement of the double bonds in the rings of the two molecules in terms of photostability in the matrix. It is found that 1,4-cyclohexadiene, which is  $\gamma$ -terpinene's parent molecule, shows a complex photochemistry in solution and in the gas phase;<sup>40</sup> however, there are no reported studies of its photochemistry in cryomatrices. To the best of our knowledge, there are no examples of molecules with the 1,4-hexadiene moiety isolated in matrix that are reactive upon irradiation at  $\lambda > 200$  nm. For example, attempts to introduce photochemical transformations in matrix-isolated  $\gamma$ -pyrone<sup>41</sup> were unsuccessful.

In order to identify the photoproduct(s) of the UV-C irradiated matrix-isolated  $\alpha$ -phellandrene, the spectral region of the  $\text{C}=\text{C}$  stretching modes ( $1550$ – $1700$   $\text{cm}^{-1}$ ) was first examined (Figure 7). The observed spectroscopic changes in this spectral region indicate a rearrangement of the  $\pi$ -system of the molecule after reaction. The strong  $\nu(\text{C}=\text{C})$  band observed in the spectrum of  $\alpha$ -phellandrene at  $1663$   $\text{cm}^{-1}$  as well as the less intense band at  $1601$   $\text{cm}^{-1}$ , assigned respectively to the antisymmetric and symmetric stretching vibrations of the conjugated  $\text{C}=\text{C}$  bonds, considerably decrease in intensity, being replaced by bands at  $1642$ ,  $1624$ , and  $1583$   $\text{cm}^{-1}$ . The number of new bands in this spectral region points to a photoproduct structure that contains an additional double bond compared to  $\alpha$ -phellandrene, thus being in agreement with the photoconversion of the compound into an open ring species bearing the 1,3,5-hexatriene skeleton.

The analysis of the  $1010$ – $760$   $\text{cm}^{-1}$  spectral range (Figure 7) presents further support for this conclusion. For example, the strong IR band of  $\alpha$ -phellandrene at ca.  $795$   $\text{cm}^{-1}$  due to the  $\omega(\text{C}_7\text{H}_{22})$  out-of-plane wagging mode of the  $\text{C}_8=\text{C}_7-\text{H}$  ring

fragment, decreases upon irradiation, whereas new bands at ca.  $900$   $\text{cm}^{-1}$  and in the  $967$ – $990$   $\text{cm}^{-1}$  range increase. The new bands are ascribable to the  $\text{CH}$  out-of-plane wagging mode of the rearranged  $\text{C}=\text{C}_8-\text{C}_7\text{H}=\text{C}$  fragment and the wagging vibration of the  $=\text{CH}_2$  terminal group (at  $\text{C}_6$  position) of the open-ring isomeric photoproduct, 3,7-dimethylocta-1,3,5-triene (abbreviated hereafter as DOT, see Figure 8 and Figure S3 in the Supporting Information). These new bands also appear at similar wavenumbers to those previously observed for the related compound 2,5-dimethyl-1,3,5-hexatriene isolated in an argon matrix as well as 1,3,5-hexatriene in the gas phase.<sup>42</sup>

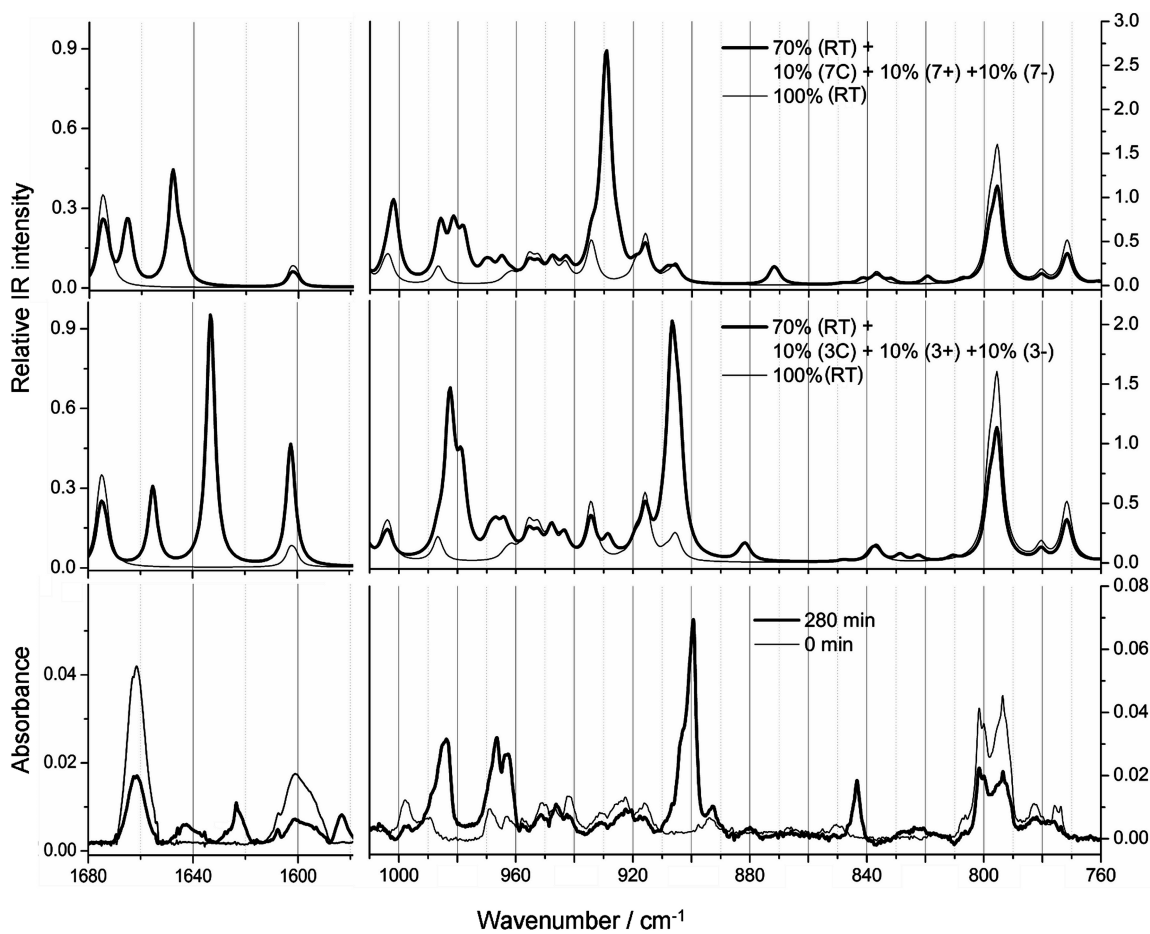
In an attempt to identify more precisely the resulting photo-products of matrix-isolated  $\alpha$ -phellandrene subjected to UV-C irradiation, we performed an extensive series of theoretical calculations on the various possible open-ring isomers of DOT.

The basis of the nomenclature here used to name the possible DOT species have been described in detail elsewhere.<sup>12</sup> Quickly, the capital letters Z or E define the configuration around the two central  $\text{C}=\text{C}$  bonds of the molecule. For each possible Z/E combination around these bonds, nine reference structures can be devised, with trans (t) or gauche (g+; g-) arrangements of the two  $\text{C}=\text{C}-\text{C}=\text{C}$  moieties (see Figure 8 and Figure S3 in the Supporting Information, which contains the full set of reference structures for DOT). Each reference structure was allowed to have three different arrangements of the isopropyl group (according to the conformation defined by the  $\text{H}-\text{C}_4-\text{C}_2-\text{C}_6$  dihedral: cis ( $0^\circ$ ; C), skew+ ( $+120^\circ$ ; SK+), and skew- ( $-120^\circ$ ; SK-)). Hence, the molecular conformations of DOT can be uniquely described by combinations of five letters, which define the arrangements around the conformationally relevant bonds of the  $\text{H}_2\text{C}=\text{C}-\text{C}=\text{C}-\text{C}=\text{C}-\text{CH}(\text{CH}_3)_2$  backbone, starting from the left to the right.

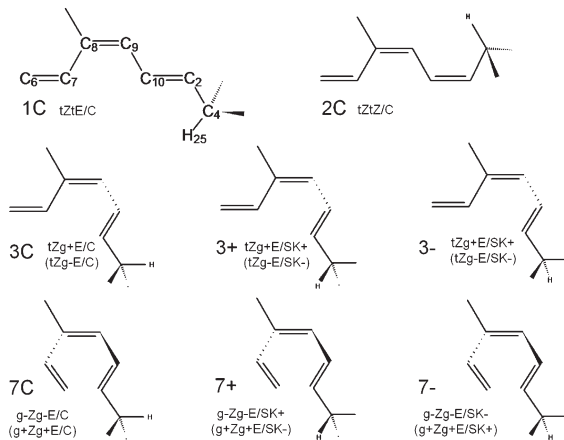
Thirty-eight different minima could be found on the PES of DOT, corresponding to 14 ZE-type structures, 5 ZZ-type structures, 14 EE-type structures, and 5 EZ-type structures. For simplicity, the minimum energy structures are named here using the notation of the closest resembling reference structure represented in Figure S3 (Supporting Information). The minimum-energy structures and their defining dihedral angles, dipole moments, and relative energies are given in Table 2. The extended tEtE/C and tZtE/C forms were predicted by the calculations to be the most stable species.

Figure 9 shows the theoretical spectra of  $\alpha$ -phellandrene and of its open-ring isomers calculated at the B3LYP/6-311++G(d,p) level of theory. The  $1800$ – $400$   $\text{cm}^{-1}$  spectral region can be used as a spectral marker for discriminating different isomers taking into account their characteristic strong infrared absorbances, particularly those related with the out-of-plane vibrations of the two central CH groups in the  $1000$ – $800$   $\text{cm}^{-1}$  range. Besides open-ring isomers, Figure 9 also shows the calculated spectra and possible structures for the Dewar isomer of  $\alpha$ -phellandrene (top frame). The Dewar isomer, which might exist in three different conformational states differing by the orientation of the isopropyl substituent, has been considered in this analysis by the analogy with the photochemistry of  $\alpha$ -pyrone.<sup>38</sup>

The Dewar isomer of  $\alpha$ -phellandrene is predicted to give rise to an intense band (due to the out-of-plane bending vibration of the CH groups attached to the central  $\text{C}=\text{C}$  bond) at ca.  $830$   $\text{cm}^{-1}$ . In the experimental spectra of the photolyzed matrix, such band does not exist (see Figure 7), which indicates that the Dewar form is not formed upon irradiation of matrix-isolated



**Figure 7.** (Bottom) Experimental FTIR spectra of  $\alpha$ -phellandrene in an argon matrix in the ranges  $1680\text{--}1620\text{ cm}^{-1}$  (concentrated sample) and  $1010\text{--}760\text{ cm}^{-1}$  (diluted sample), before (0 min) and after UV ( $\lambda > 200\text{ nm}$ ) irradiation (280 min). (Middle and Top) Theoretical infrared spectrum of the equilibrium mixture of the conformers at room temperature (100% RT) simulates the substrate absorption. In the simulation of the spectrum upon irradiation, the RT spectrum was reduced to 70%, and the resulting scaled spectrum was coadded with the spectrum of the putative open-ring product (3 $-$ , 3 $+$ , 3C or 7 $-$ , 7 $+$ , 7C), which was reduced to 30%. The abbreviated names 3 $+$ , 3 $-$ , and 3C stand for the tZg+E/SK+, tZg+E/SK $-$ , and tZg+E/C, and names 7 $+$ , 7 $-$ , and 7C stand for the g-Zg-E/SK+, g-Zg-E/SK $-$ , and g-Zg-E/C conformers of the photoproduct (see also Table 2 and Figure 9). The theoretical spectra were simulated by Lorentzian functions centered at the DFT(B3LYP)/6-311++G(d,p) calculated wavenumbers scaled by 0.978 and with fwhm equal to  $4\text{ cm}^{-1}$  (see also Figure 8 and Figure S3 in the Supporting Information).



**Figure 8.** Selected reference structures and notation adopted to name the possible isomeric structures and conformers of DOT. The names of symmetry-equivalent mirror images reference structures are given in parentheses. Figure S3 (Supporting Information) shows the full set of considered reference structures of DOT.

$\alpha$ -phellandrene. This result parallels that found previously for  $\alpha$ -terpinene.<sup>12</sup>

Because in Figure 9 the ordinate scales are equal in all frames, one can easily notice that the infrared intensities of the open-ring photoproducts are larger than in the starting compound. The main observations and conclusions extracted from this figure, aside from the nonproduction of the Dewar isomer, are the following:

- (i) In the theoretical spectra of EE-type DOT forms (8, 10, 11, 13, 14) intense bands are predicted at about  $900$  and  $1700\text{ cm}^{-1}$ ;
- (ii) In the theoretical spectra of EZ-type DOT forms (9, 12) intense bands are predicted at about  $800$  and  $900\text{ cm}^{-1}$ ;
- (iii) In the theoretical spectra of ZZ-type DOT forms (2, 5) intense bands are predicted at about  $800$  and  $1000\text{ cm}^{-1}$ ;
- (iv) In the theoretical spectra of ZE-type DOT forms (1, 3, 4, 6, 7) intense bands are predicted at about  $900$  and  $1000\text{ cm}^{-1}$ .

Since each type of configuration about the two central double bonds in DOT has a characteristic signature, comparison of these signatures with the experimental data (IR spectrum of the photolyzed

**Table 2. Structural and Energetic Parameters of  $\alpha$ -Phellandrene Conformers and of the Corresponding Open-Ring Isomers Calculated at the DFT(B3LYP)/6-311++G(d,p) Level of Theory<sup>a</sup>**

name	short name	dihedral angles					$ \mu $	relative energy		
		A	B	C	D	E		$\Delta E^\circ$	$\Delta E_{\text{ZPVE}}^\circ$	$\Delta G^\circ$
trans	T					179.6	0.23	0.00	0.00	0.00
gauche-	G-					-48.1	0.29	0.42	0.37	0.27
gauche+	G+					69.6	0.21	0.80	1.00	1.06
tZtE/C	1C	180.0	0.0	180.0	180.0	0.0	0.57	35.1	27.7	20.6
tZtE/SK+	1+	180.0	0.2	-179.8	179.7	120.3	0.73	38.4	31.7	25.3
tZtZ/C	2C	180.0	0.0	180.0	0.0	0.0	0.60	41.9	35.5	27.2
tZtZ/SK+	2+	179.9	0.2	179.9	-0.1	129.8	0.75	59.2	54.1	46.7
tZg+E/C	3C	-172.0	5.6	39.9	178.8	-0.4	0.50	51.8	44.7	37.9
tZg+E/SK+	3+	-171.9	5.7	41.0	178.5	121.6	0.56	55.2	48.7	42.9
tZg+E/SK-	3-	-172.1	5.7	41.2	179.1	-120.2	0.60	55.4	48.9	43.1
g-ZtE/C	4C	-45.4	-3.8	176.1	178.3	0.2	0.08	49.1	40.7	33.1
g-ZtE/SK+	4+	-45.6	-3.8	176.7	177.8	120.5	0.16	52.4	44.7	38.0
g-ZtE/SK-	4-	-45.6	-3.8	176.8	178.6	-120.5	0.22	52.4	45.0	38.7
g-ZtZ/C	5C	-44.2	-4.5	173.2	-3.2	1.3	0.44	55.4	47.8	39.7
g-ZtZ/SK+	5+	-43.6	-4.7	171.1	-4.5	131.1	0.38	72.2	66.2	59.1
g-ZtZ/SK-	5-	-43.7	-4.9	171.8	-3.8	-127.7	0.36	72.0	65.7	58.1
g-Zg+E/C	6C	-65.1	-2.2	41.6	-179.8	0.5	0.18	77.6	68.9	60.6
g-Zg+E/SK+	6+	-65.5	-2.2	42.6	-179.9	120.9	0.24	81.5	73.3	65.1
g-Zg+E/SK-	6-	-66.2	-2.0	43.1	-179.5	-120.9	0.14	81.7	73.6	65.4
g-Zg-E/C	7C	-55.2	-5.4	-41.1	-177.5	0.5	0.14	75.0	65.3	56.2
g-Zg-E/SK+	7+	-56.1	-5.3	-41.7	-178.0	121.1	0.30	78.6	70.2	63.0
g-Zg-E/SK-	7-	-54.6	-5.2	-42.6	-178.2	-119.5	0.26	78.1	69.1	61.3
tEtE/C	8C	180.0	180.0	180.0	180.0	0.0	0.95	31.7	24.3	17.1
tEtE/SK+	8+	180.0	179.9	179.7	179.6	120.2	1.05	35.0	27.9	21.3
tEtZ/C	9C	180.0	180.0	180.0	0.0	0.0	0.53	38.4	31.6	22.2
tEtZ/SK+	9+	180.0	-179.8	179.6	-0.3	130.2	0.77	55.4	49.9	42.1
tEg-E/C	10C	-177.1	178.3	-35.7	-178.6	-1.2	0.91	49.5	42.5	36.0
tEg-E/SK+	10+	-177.1	178.4	-36.5	-179.0	119.5	1.03	53.4	46.9	40.9
tEg-E/SK-	10-	-177.3	178.6	-36.6	-178.5	-122.1	1.04	53.2	46.8	40.8
g-EtE/C	11C	-34.0	178.2	178.7	179.7	0.2	0.65	46.0	37.5	29.0
g-EtE/SK+	11+	-34.0	178.3	178.9	179.4	121.2	0.70	49.3	41.4	33.6
g-EtE/SK-	11-	-34.1	178.2	178.8	180.0	-120.4	0.70	49.4	41.5	33.8
g-EtZ/C	12C	-34.4	177.9	178.3	-0.3	1.5	0.15	52.5	44.7	34.9
g-EtZ/SK+	12+	-34.4	177.9	177.6	-0.7	129.2	0.35	69.4	63.0	54.1
g-EtZ/SK-	12-	-34.2	177.5	177.6	-0.3	-128.4	0.36	69.5	63.2	54.5
g-Eg-E/C	13C	-36.9	177.7	-34.0	-179.1	-0.7	0.73	61.6	53.9	46.9
g-Eg-E/SK+	13+	-37.4	177.8	-35.2	-179.6	120.2	0.86	65.5	58.0	51.3
g-Eg-E/SK-	13-	-37.2	177.8	-35.3	-178.9	-122.0	0.88	65.2	58.0	51.6
g-Eg+E/C	14C	-34.8	179.5	33.2	178.6	0.2	0.61	65.1	56.8	47.9
g-Eg+E/SK+	14+	-35.0	179.4	37.2	178.4	121.9	0.76	68.8	61.2	54.1
g-Eg+E/SK-	14-	-35.3	179.5	36.5	179.0	-120.1	0.74	69.0	61.1	53.4

<sup>a</sup> DFT(B3LYP)/6-311++G(d,p) calculated energies of the closed-ring trans conformer of  $\alpha$ -phellandrene was chosen as the zero level. The relative calculated energies of the remaining forms are given in kJ mol<sup>-1</sup>. The absolute energies of T conformer are given in the caption of Table 1. Dipole moments ( $|\mu|$ /debye). Dihedral angles A, B, C, D, E (degrees) stand for  $C_6=C_7-C_8=C_9$ ,  $C_7-C_8=C_9-C_{10}$ ,  $C_8=C_9-C_{10}=C_2$ ,  $C_9-C_{10}=C_2-C_4$  (isopropyl side), and  $C_{10}=C_2-C_4-H_{25}$  (isopropyl). For the closed-ring molecule, the values of dihedral angle E (defining orientation of the isopropyl group) refer to the  $H_2C-C-C-H$  angle. In the abbreviated names, the backbone structure is designated by an arabic numeral followed by + (skew+), - (skew-) or C (cis), defining the orientation of isopropyl group.

$\alpha$ -phellandrene matrix; see Figure 7) was carried out in an attempt to identify the isomers resulting from the observed photochemical reaction. In the spectrum of the irradiated matrix, prominent bands due to the photoproduct are observed at about 900 and 1000 cm<sup>-1</sup>,

thus allowing to conclude that the observed photochemistry leads to the predominant formation of the ZE-isomer of DOT.

Comparison of the spectra of the different conformers of a given type of isomeric structures sharing the same configuration about

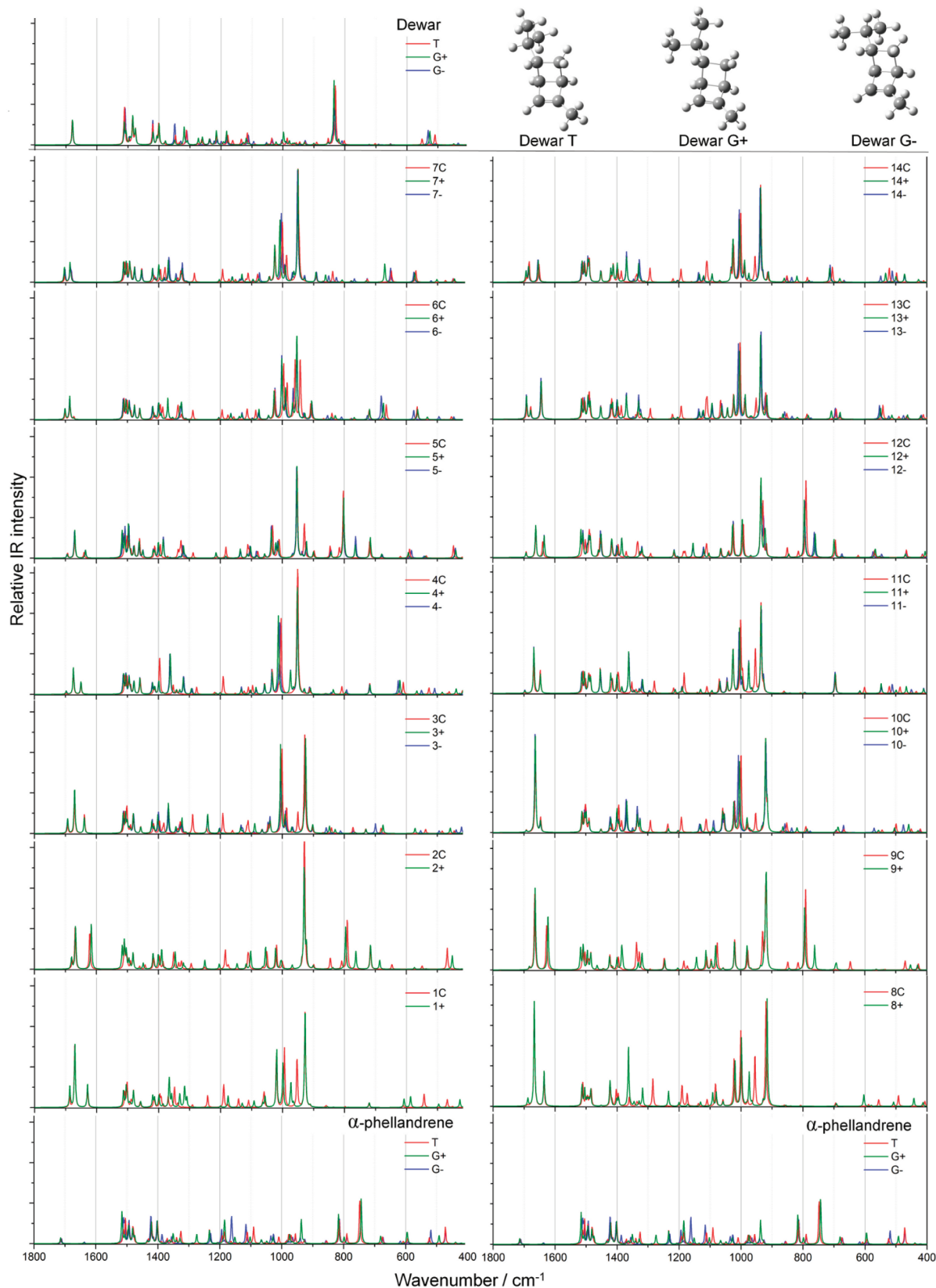


**Figure 9.** Theoretical spectra of  $\alpha$ -phellandrene (bottom frame) and its possible isomers calculated at the DFT(B3LYP)/6-311++G(d,p) level of approximation (see Figure S3 in the Supporting Information). The calculated frequencies and intensities are not scaled. Note that ordinate scales are equal in all frames.

the two central C=C bonds shows that they are very similar. Therefore, the identification of the particular conformer(s) generated in

the photoreaction is difficult. However, simulations of infrared spectral changes occurring upon photolysis were made assuming

the different sets of conformers sharing the common *ZE*-configuration as possible photoproducts. Based on the close match between the experimentally observed spectroscopic changes upon irradiation and the simulation resulting when open-ring isomers with the *tZgE* and *gZgE* backbone were used (see Figure 7), the most likely conformers of DOT resulting from photolysis of matrix isolated  $\alpha$ -phellandrene seem to be those exhibiting this backbone, i.e., 3C, 3+, 3- and 7C, 7+, 7-. These conformers require the smallest structural rearrangement of both the reactant and surrounding matrix, thus being in concordance with the principle of least motion,<sup>43</sup> which has been formulated in the context of the ring-opening reaction in related compounds, and proved to be obeyed by the analogous molecule,  $\alpha$ -terpinene.<sup>12</sup> The expected mechanism of the photoprocess is a concerted  $\sigma^2 + \pi^4$  electrocyclic ring-opening conrotatory reaction taking place in  $S_1$  (according to the Woodward–Hoffmann orbital symmetry rules<sup>44</sup>), closely resembling that proposed for  $\alpha$ -terpinene.<sup>12</sup>

The sole production of *ZE*-type conformers of the photo-product of  $\alpha$ -phellandrene is in line with the photochemistry of matrix-isolated 1,3-cyclohexadiene, which was found to undergo rapid photolysis exclusively to a specific type of open-chain structure (*Z* forms in that case),<sup>45</sup> but with different isopropyl group orientations. This is in agreement with NEER principle (nonequilibration of excited rotamers), which notes that equilibration of the excited rotamers during the singlet-excited-state lifetime does not occur, implying unique photochemistry and photophysics for each rotamer<sup>42</sup>). For  $\alpha$ -phellandrene, if the photoisomerization of each conformer is highly stereoselective giving the product anticipated in a model emphasizing ground-state geometry as a stereochemical determinant and accounting for the principle of least motion,<sup>43</sup> then two different conformers with a given backbone type and different isopropyl group orientation should be produced from each conformer of the reactant (for CCW and CW rotation of the isopropyl fragment). On the whole, all six *tZgE*-type or *gZgE*-type conformers of DOT would then be produced. This is in agreement with the spectroscopic data shown in Figure 7, showing that structures 3C, 3+, 3- as well as 7C, 7+, 7- exhibit infrared spectra that are congruous with the experimental spectrum of the photoproduct.

## CONCLUSIONS

This paper compares molecular structures and photochemical properties of  $\gamma$ -terpinene and  $\alpha$ -phellandrene which are two structural monoterpenes isomers with 1,4- and 1,3-diene six-membered rings, respectively. The conformational space of the two compounds was fully characterized using DFT calculations. Each molecule can adopt three conformations related with the internal rotation of the exocyclic isopropyl group. The potential energy profiles for interconversion between conformers were also characterized. For both compounds, the gas-phase conformational population characteristic of room temperature (RT) could be efficiently trapped in cryogenic Ar matrices. High energy barriers (at least 15 kJ mol<sup>-1</sup>) separating the unique conformers prevent conformational relaxation during the matrix deposition. The signatures of all conformers were identified in the experimental IR spectra with the lowest energy trans forms dominating for both matrix-isolated compounds. The FTIR-ATR spectrum of liquid  $\alpha$ -phellandrene and  $\gamma$ -terpinene and the IR spectra obtained for the compounds isolated in argon matrices show only minor differences. The comparison between the experimental FT-Raman spectra of  $\alpha$ -phellandrene and  $\gamma$ -terpinene at RT and the theoretical Raman spectra of their conformers in the

1200–1000 cm<sup>-1</sup> region shows that conformational population in the liquid phase at RT is comparable with the population in the gas phase at RT. Moreover, Raman spectroscopy aided in the conformational characterization of the studied compounds providing the experimental frequencies for the vibrations that are weakly absorbing in infrared but have high Raman activities, in agreement with the DFT calculations.

Vibrational analysis of the matrix spectra was focused on the conformer-specific regions corresponding to the C=C stretching and C–H bending vibrations. These spectral regions, 1700–1600 and 1200–760 cm<sup>-1</sup>, were especially sensitive to the photochemical changes in the studied molecules. These changes are related with reorganization of the  $\pi$ -system in the course of the UV-induced photoreaction. Upon irradiation at  $\lambda > 200$  nm, no change was observed in the spectrum of  $\gamma$ -terpinene, while new bands emerged in the spectrum of  $\alpha$ -phellandrene. These results show that  $\alpha$ -phellandrene is photolabile under germicidal UV-C light and demonstrate the relevance of the different double bonds arrangement in the two rings on their photostability. The observed photoprocess for  $\alpha$ -phellandrene is a typical concerted electrocyclic ring-opening reaction. The series of theoretical calculations (which were carried out on the whole set of possible open-ring isomers of  $\alpha$ -phellandrene) and analysis of the spectra of the irradiated matrices suggest that the most likely photoproducts are the open-ring isomers with the *tZgE* backbone, i.e., those that require the smallest changes of the reacting species as well as the smallest changes of the local environment.

## ASSOCIATED CONTENT

**S Supporting Information.** Figure S1, showing the comparison of the FT-Raman spectra of liquid  $\alpha$ -phellandrene and  $\gamma$ -terpinene at 298 K with the simulated Raman spectra for their conformers; Figure S2, with the UV–vis spectra of 10<sup>-4</sup> M ethanol solutions of  $\alpha$ -terpinene,  $\alpha$ -phellandrene, and  $\gamma$ -terpinene; Figure S3, showing the reference structures and notation adopted to name the open-ring isomers of  $\alpha$ -phellandrene; Table S1, presenting the structural parameters of the conformers of  $\alpha$ -phellandrene and  $\gamma$ -terpinene calculated at the DFT(B3LYP)/6-311++G(d,p) level of theory; Tables S2, S4, and S6, with the definition of internal coordinates used in the normal coordinate analysis calculations for  $\alpha$ -phellandrene,  $\gamma$ -terpinene, and DOT (*tZgE* form), respectively; Tables S3, S5, and S7, presenting the experimental wavenumbers and intensities (qualitative) of the infrared spectra  $\alpha$ -phellandrene,  $\gamma$ -terpinene, and DOT (*tZgE* form), respectively, as well as the calculated infrared spectra for the relevant conformers of each molecule and potential energy distributions resulting from the normal coordinate analysis calculations. This material is available free of charge via the Internet at <http://pubs.acs.org>.

## AUTHOR INFORMATION

### Corresponding Author

\*E-mail: proniewi@chemia.uj.edu.pl (L.M.P.); rfausto@ci.uc.pt (R.F.). Phone: +48 12 663 2288 (L.M.P.); +351 91 9236971 (R.F.).

## ACKNOWLEDGMENT

This work was supported by The Polish State Committee for Scientific Research, 2009/2011 (Grant No. N N204 341437),

the Portuguese “Fundação para a Ciéncia e a Tecnologia”, FCT (Projects PTDC/QUI/71203/2006 and PTDC/QUI-QUI/111879/2009, also supported by QREN-FEDER/COMPETE), and the European Union from the resources of the European Regional Development Fund under the Innovative Economy Programme (grant coordinated by JCET-UJ, No POIG.01.01.02-00-069/09).

## ■ REFERENCES

- (1) Shaw, P. E.; Moshonas, M. G.; Bowman, K. D. *Phytochemistry* **2000**, *53*, 1083–1086.
- (2) Jacobs, S. W. L.; Pickard, J. *Plants of New South Wales*; Government Printing: Sydney, NSW, Australia, 1981; ISBN 0-7240-1978-2.
- (3) Pongprayoon, U.; Soontorn saratun, P.; Jarikasem, S.; Sematong, T.; Wasuwat, S.; Claeson, P. *Phytomedicine* **1996/97**, *3*, 319–22.
- (4) Williams, A. C.; Barry, B. W. *Pharm. Res.* **1991**, *8*, 17–24.
- (5) Al-Burtamani, S. K. S.; Fatope, M. O.; Marwah, R. G.; Onifade, A. K.; Al-Saidi, A. S. H. *J. Ethnopharmacol.* **2005**, *96*, 107–112.
- (6) Cheng, S.; Liu, J.; Hsui, Y.; Chang, S. *Bioresour. Technol.* **2006**, *97*, 306–312.
- (7) Nhu-Trang, T.; Casabianca, H.; Grenier-Loustalot, M. *J. Chromatogr. A* **2006**, *1132*, 219–227.
- (8) Schulz, H.; Barańska, M. *Vibrat. Spectrosc.* **2007**, *43*, 13–25.
- (9) Schulz, H.; Özkan, G.; Barańska, M.; Kruger, H.; Özcan, M. *Vibrat. Spectrosc.* **2005**, *39*, 249–259.
- (10) Breitmaier, E. *Terpenes: Flavors, Fragrances, Pharmaca, Pheromones*; Wiley-VCH: Weinheim, Germany, 2006.
- (11) Bond, A. D.; Davies, J. E. *Acta Crystallogr.* **2001**, *57*, 1032–1033.
- (12) Marzec, K. M.; Reva, I.; Fausto, R.; Malek, K.; Proniewicz, L. M. *J. Phys. Chem. A* **2010**, *114*, 5526–5536.
- (13) Harkenthal, M.; Reichling, J.; Geiss, H. K.; Saller, R. *Pharm. Z.* **1998**, *143*, 26–30.
- (14) Gallivan, J. B.; Brinen, J. S. *Chem. Phys. Lett.* **1971**, *10*, 455–459.
- (15) Iwanami, Y.; Tateba, H.; Kodama, N.; Kishino, K. *J. Agric. Food Chem.* **1997**, *45*, 463–466.
- (16) Land, E. J.; Truscott, T. G. *Photochem. Photobiol.* **1979**, *29*, 861–886.
- (17) Hausen, B. M.; Reichling, J.; Harkenthal, M. *Am. J. Contact Dermat.* **1999**, *10*, 68–77.
- (18) Avcibaşı, N.; İçli, S.; Gilbert, A. *Turk. J. Chem.* **2003**, *27*, 1–7.
- (19) Garavelli, M.; Page, C. S.; Celani, P.; Olivucci, M.; Schmid, W. E.; Trushin, S. A.; Fuss, W. *J. Phys. Chem. A* **2001**, *105*, 4458–4469.
- (20) Dou, Y.; Yuan, S.; Lo, G. V. *Appl. Surf. Sci.* **2007**, *253*, 6404–6408.
- (21) Fuss, W.; Schikarski, T.; Schmid, W. E.; Trushin, S.; Kompa, K. L. *Chem. Phys. Lett.* **1996**, *262*, 675–682.
- (22) Kauffmann, E.; Frei, H.; Mathies, R. A. *Chem. Phys. Lett.* **1997**, *266*, 554–559.
- (23) Dudek, R. C.; Weber, P. M. *J. Phys. Chem. A* **2001**, *105*, 4167–4171.
- (24) Reid, P. J.; Doig, S. J.; Wickham, S. D.; Mathies, R. A. *J. Am. Chem. Soc.* **1993**, *115*, 4754–4763.
- (25) (a) Geppert, D.; Seyfarth, L.; De Vivie-Riedle, R. *Appl. Phys. B: Lasers Opt.* **2004**, *79*, 987–992. (b) Ruan, C.-Y.; Lobastov, V. A.; Srinivasan, R.; Goodson, B. M.; Ihhee, H.; Zewail, A. H. *Proc. Natl. Acad. Sci. U.S.A.* **2001**, *98*, 7117–7122. (c) Kurtz, L.; Hofmann, A.; de Vivie-Riedle, R. *J. Chem. Phys.* **2001**, *114*, 6151–6159.
- (26) (a) de Kock, R. J.; Minnaard, N. G.; Havinga, E. *Recl. Trav. Chim. Pays-Bas.* **1960**, *79*, 922–934. (b) Crowley, K. J.; Erickson, K. L.; Eckell, A.; Meinwald, J. *J. Chem. Soc., Perkin Trans. 1* **1973**, 2671–2679. (c) Reid, P. J.; Doig, S. J.; Mathies, R. A. *J. Phys. Chem.* **1990**, *94*, 8396–8399.
- (27) Climent, M. J.; Miranda, M. A.; Roth, H. D. *Eur. J. Org. Chem.* **2000**, 1563–1567.
- (28) Frisch, M. J.; Trucks, G. W.; Schlegel, H. B.; Scuseria, G. E.; Robb, M. A.; Cheeseman, J. R.; Scalmani, G.; Barone, V.; Mennucci, B.; Petersson, G. A.; Nakatsuji, H.; Caricato, M.; Li, X.; Hratchian, H. P.; Izmaylov, A. F.; Bloino, J.; Zheng, G.; Sonnenberg, J. L.; Hada, M.; Ehara, M.; Toyota, K.; Fukuda, R.; Hasegawa, J.; Ishida, M.; Nakajima, T.; Honda, Y.; Kitao, O.; Nakai, H.; Vreven, T.; Montgomery, Jr., J. A.; Peralta, J. E.; Ogliaro, F.; Bearpark, M.; Heyd, J. J.; Brothers, E.; Kudin, K. N.; Staroverov, V. N.; Kobayashi, R.; Normand, J.; Raghavachari, K.; Rendell, A.; Burant, J. C.; Iyengar, S. S.; Tomasi, J.; Cossi, M.; Rega, N.; Millam, N. J.; Klene, M.; Knox, J. E.; Cross, J. B.; Bakken, V.; Adamo, C.; Jaramillo, J.; Gomperts, R.; Stratmann, R. E.; Yazyev, O.; Austin, A. J.; Cammi, R.; Pomelli, C.; Ochterski, J. W.; Martin, R. L.; Morokuma, K.; Zakrzewski, V. G.; Voth, G. A.; Salvador, P.; Dannenberg, J. J.; Dapprich, S.; Daniels, A. D.; Farkas, Ö.; Foresman, J. B.; Ortiz, J. V.; Cioslowski, J.; Fox, D. J. *Gaussian 09, Revision A.1*; Gaussian, Inc.: Wallingford, CT, 2009.
- (29) Lee, C.; Yang, W.; Parr, R. G. *Phys. Rev. B* **1988**, *37*, 785–789.
- (30) Cossi, M.; Scalmani, G.; Rega, N.; Barone, V. *J. Chem. Phys.* **2002**, *117*, 43–54.
- (31) Cossi, M.; Rega, N.; Scalmani, G.; Barone, V. *J. Comput. Chem.* **2003**, *24*, 669–681.
- (32) Michalska, D.; Wysokinski, R. *Chem. Phys. Lett.* **2005**, *403*, 211–217.
- (33) Reva, I.; Lopes Jesus, A. J.; Rosado, M. T. S.; Fausto, R.; Eusébio, M. E.; Redinha, J. S. *Phys. Chem. Chem. Phys.* **2006**, *8*, 5339–5349.
- (34) Andrzejewska, A.; Lapinski, L.; Reva, I.; Fausto, R. *Phys. Chem. Chem. Phys.* **2002**, *4*, 3289–3296.
- (35) Fogarasi, G.; Zhou, X.; Taylor, P. W.; Pulay, P. *J. Am. Chem. Soc.* **1992**, *114*, 8191–8201.
- (36) Pulay, P.; Fogarasi, G.; Pang, F.; Boggs, J. E. *J. Am. Chem. Soc.* **1979**, *101*, 2550–2560.
- (37) Martin, J. M. L.; Van Alsenoy, C. *Gar2ped*; University of Antwerp: Antwerp, Belgium, 1995.
- (38) Breda, S.; Reva, I. D.; Lapinski, L.; Fausto, R. *Phys. Chem. Chem. Phys.* **2004**, *6*, 929–937.
- (39) Harris, D. A.; Orozco, M. B.; Sension, R. J. *J. Phys. Chem. A* **2006**, *110*, 9325–9333.
- (40) White, L. S.; Rossi, A. R.; Epling, G. A. *J. Am. Chem. Soc.* **1981**, *103*, 7299–7304.
- (41) Seixas de Melo, J.; Quinteiro, G.; Pina, J.; Breda, S.; Fausto, R. *J. Mol. Struct.* **2001**, *59*, 565–566.
- (42) (a) Brouwer, A. M.; Jacobs, H. J. C. *Recl. Trav. Chim. Pays-Bas.* **1995**, *114*, 449–458. (b) Craig, N. C.; Leyden, M. C.; Moore, M. C.; Patchen, A. K.; Van den Heuvel, T.; Blake, T. A.; Masiello, T.; Sams, R. L. *J. Mol. Spectrosc.* **2010**, *262*, 49–60.
- (43) Baldwin, J. E.; Krueger, S. M. *J. Am. Chem. Soc.* **1969**, *91*, 6444–6447.
- (44) Woodward, R. B.; Hoffmann, R. *The Conservation of Orbital Symmetry*; Verlag Chemie: Weinheim, Germany, 1970.
- (45) Danen, W. C.; Tipton, T. J.; Saunders, D. G. *J. Am. Chem. Soc.* **1971**, *93*, 5186–5189.